DALTON

Investigation of the bonding in methyl titanium trichloride by variable-energy photoelectron spectroscopy and density functional calculations*

Christian N. Field,[a] Jennifer C. Green,[a] Nikolas Kaltsoyannis,[b] G. Sean McGrady,[a] Aidan N. Moody,[a] Michele Siggel[c] and Monica De Simone[a]

[a] *Inorganic Chemistry Laboratory, South Parks Road, Oxford OX1 3QR, UK*
[b] *Department of Chemistry, University College, London, 20 Gordon Street, London WC1H 0AJ, UK*
[C] *EPSRC Daresbury Laboratory, Daresbury, Warrington WA4 4AD, UK*

Preparation of an authentically pure sample of [$TiMeCl_3$] has enabled measurement of its photoelectron spectrum with photon energies varying between 20 and 50 eV. Study of the relative partial photoionisation cross-sections of the valence photoelectron bands has enabled a full assignment of the related ion states. The character of the ionising orbitals was also deduced from the cross-section variations. The titanium–carbon bond was shown to have a significant Ti 3d character. Density functional calculations at the non-local level, including estimates of the ionisation energies using Slater's transition-state method, are in good agreement as to the ion state ordering. Fragment analysis of the one-electron eigenfunctions is fully consistent with the experimentally deduced orbital character.

The past decade has witnessed intensive efforts to understand the structure and bonding in the fundamentally important compound methyl titanium trichloride, [$TiMeCl_3$] **1**. A report in 1986 concluded that the methyl group in **1** was significantly distorted as the result of an agostic interaction with the titanium centre.[1] This was on the basis of a gas-phase electron-diffraction study, with supporting evidence coming from anomalies in the vibrational spectrum of the vapour and remarkable values for the solution NMR parameters $\delta(^{13}C)$ and $^2J(HH)$. All the evidence pointed to abnormal hybridisation at the carbon atom and a flattened methyl moiety with anomalously long C–H bonds.

These results appeared to tally with the crystal structure of the adduct [$TiMeCl_3$]·dmpe **2** (dmpe = $Me_2PCH_2CH_2PMe_2$), which indicated a highly distorted TiMe moiety and an unusually short Ti···H distance.[2] In 1988 the crystal structure of **1** showed the compound to be dimeric in the solid state with chloride bridges and highly distorted methyl groups. This geometry was also interpreted in terms of an agostic Ti···H–C interaction.[3] Since this report, however, substantial reinvestigation has occurred. The gas-phase electron-diffraction pattern of **1** was redetermined, and showed the geometry to be more-or-less normal.[4] Remeasurement of $^2J(HH)$ also led to the conclusion that there was nothing anomalous about the methyl group.[5] An infrared study of several isotopomers of [$TiMeCl_3$] showed abnormally low $\delta(CH_3)$ and $\rho(CH_3)$ frequencies but the remaining vibrations of the methyl group were normal for an organometallic compound and the ν(CH) and ν(CD) frequencies were consistent with an unexceptional methyl geometry.[6] Hartree–Fock and (MP2) second-order Moeller-Plesset perturbation calculations on **1** and the model compound [$TiMeH_3$] led to the conclusion that the anomalies in the vibrational spectrum were caused by the nature of the Ti–C, rather than the C–H, bonding.[7] An all-electron MP2 study of **1** provided a theoretical structure as well as vibrational frequencies in excellent agreement with the revised experimental data.[8] The ^{13}C NMR data were similarly reinterpreted.[9] Thus the only remaining evidence for an abnormal methyl group geometry in [$TiMeCl_3$] rests with the solid-state structures of **1** and **2**.

An early study of the He I and He II photoelectron spectrum of compound **1** concluded that there were 'striking similarities between the spectra of [$TiMeCl_3$] and $TiCl_4$'.[10] In view of our experience regarding the difficulty in obtaining **1** rigorously pure (see Experimental section), suspicions must arise about the integrity of the sample in this earlier report. We, therefore, report below the photoelectron spectrum of an authentic sample of **1**.

The structure and bonding of the heavy-atom skeleton is also of considerable interest with regard both to the involvement of the atomic orbitals on titanium, and to the extent of π donation from the electronegative Cl ligands to the formally eight-electron d^0 titanium centre. Variable-energy photoelectron spectroscopy (PES) affords an ideal technique for assessing both of the above contributions to the bonding. The Ti 3d, Cl 3p and C 2p atomic orbitals (AOs) differ in their photoionisation cross-section variations with photon energy. Use of a synchrotron source enables PE spectral measurement with a wide range of photon energies, and consequent determination of the relative cross-sections of the PE bands enables an analysis of the AO contributions to the associated molecular orbitals (MOs).[11]

Experimental

Initial experiments were conducted to assess the purity of compound **1** produced by the literature method using dimethylzinc as the methylating agent, according to equation (1).[4] After

$$0.5\ ZnMe_2 + TiCl_4 \xrightarrow[0\ ^\circ C]{\text{isopentane}} [TiMeCl_3] \qquad (1)$$

filtration and removal of solvent at −78 °C the IR spectrum of the sample obtained always showed the presence of significant amounts of $TiCl_4$ impurity. We attribute this non-stoichiometry to the insolubility and/or reduced methylating capacity of the intermediate methylzinc chloride, ZnMeCl. Use of a 1:1 molar

* *Non-SI units employed:* eV ≈ 1.60×10^{-19} J, in = 2.54×10^{-2} m.

ratio of $ZnMe_2$ and $TiCl_4$ is known to produce substantial amounts of the higher product dimethyl titanium dichloride $[TiMe_2Cl_2]$ **3**.[12] Hence it appears that the $ZnMe_2$–$TiCl_4$–$[TiMeCl_3]$–$[TiMe_2Cl_2]$ system is complex and non-stoichiometric.

Pure compound **1** was obtained by treating $TiCl_4$ (3.16 g, 16.6 mmol) with $ZnMe_2$ (0.82 g, 8.6 mmol) in isopentane (*ca.* 50 cm^3), and by sampling the mixture by gas-phase IR spectroscopy. A solution of $ZnMe_2$ (0.60 g, 2.29 mmol) in isopentane (8.0 cm^3) was added to the reaction mixture in 0.25 cm^3 aliquots, and the resulting IR spectrum used to monitor the consumption of the excess of $TiCl_4$. A total of 1.5 cm^3 of this solution was required to remove the last traces of the tetrachloride, corresponding to an approximate 15% excess of that indicated by equation (1). The final sample was shown to be free from the potential impurities $TiCl_4$ and $[TiMe_2Cl_2]$ to a level of > 99% by a combination of IR and NMR spectroscopies.[6,13,14]

He I and He II PE spectroscopy

The He I and He II spectra of $[TiMeCl_3]$ were obtained using a PES Laboratories 0078 spectrometer, calibrated using He and Xe. The He I spectrum was fitted using eight asymmetric Gaussian curves. In the He II spectrum the positions of the two inner valence states were fixed by fitting with two symmetric Gaussian curves.

Variable-photon-energy PE spectroscopy

This experiment was carried out at the synchrotron radiation (SR) facility of the EPSRC Daresbury Laboratory. The SR was monochromated using a toroidal grating monochromator (TGM), at beamline 3.3. The TGM was used with fixed entrance and exit slit widths of 5.5 mm. One grating was employed covering the photon energy range 22–50 eV (710 lines per mm). The photons were introduced to the ionisation region *via* a glass light guide, 2 mm in diameter. The data were collected using the chemical angle resolved photoelectron spectrometer, CARPES, which is described elsewhere.[15] The photoelectrons were energy analysed using the focusing action of a three-element zoom lens to accelerate or retard them followed by a hemispherical analyser of mean radius 45 mm which was operated at a pass energy of 5.355 eV for photon energies of 22–50 eV. Total instrumental energy resolution was in the range 23–35 meV. A position-sensitive multichannel detector was used consisting of a pair of chevronned multichannel plates backed by a resistive anode. Owing to partial polarisation of the incident synchrotron radiation, the lens and analyser were positioned at the 'magic angle' with respect to the plane of polarisation of the light so that the photoionisation cross-sections, and thus intensities of the various ionisation bands, were not affected by the photoelectron asymmetry parameter, β.

The sample was introduced to the ionisation region *via* stainless-steel tubing (outside diameter ¼ in) and the vapour pressure in the chamber controlled by a needle valve in the sample line. The sample of $[TiMeCl_3]$ was stored at −80 °C until immediately before the PES experiment. The data were recorded with the sample at 0 °C and the inlet system at room temperature. A liquid-nitrogen-cooled cold-finger was used to prevent diffusion of the compound into the turbo and rotary pumps.

The decay of the electron current in the storage ring was corrected for by linking the scanning rate with the output from a photodiode positioned to intersect the photon beam after its passage through the gas cell. The sensitivity of the photodiode to different radiation energies was determined by measuring the $1s^{-1}$ PE spectrum of He and the np^{-1} PE spectra of Ar and Xe.[16]

Fluctuations in sample pressure were estimated and corrected for by recording a calibration spectrum of the compound at a constant photon energy ($h\nu$ = 30 eV) before and after every data spectrum. These calibration spectra were integrated across the whole spectrum to give a measurement of intensity. Variations in intensities between these calibration spectra were then interpreted as a measure of the pressure fluctuation of the sample.

Spectra were measured at intervals between 22 and 50 eV. We were unable to measure spectra over a greater photon-energy range as the sample had a deleterious effect on the channel plates. The results at 50 eV were of inferior quality.

Data analysis

As the PE spectrum of $[TiMeCl_3]$ contains many overlapping bands their areas could not be obtained by direct integration. The bands were deconvoluted by fitting with asymmetric Gaussian functions, the best fit being determined by a least-squares refinement.

To fix the values of the vertical ionisation energies (i.e.) we fitted the He I data without applying any restraint. Band labels are defined in Fig. 1 and Table 1. In fitting the spectra acquired with synchrotron radiation the width of each Gaussian curve was kept constant. These widths were chosen using, as a criterion, achievement of the mean best fit for all the photon energies employed.

Band H is the broadest and least well defined in shape as its onset overlaps with band G. The choice to fit it with only one asymmetric Gaussian curve is probably the main reason for the rapid fluctuation in the branching ratios (b.r.) and relative partial photoionization cross-sections (r.p.p.i.c.s.). Though the variations of bands D and E were treated separately, they probably lie too close together for their relative intensities to be disentangled. However the variation of their combined intensities is reliable.

The method of deriving b.r. and r.p.p.i.c.s. from the band intensities and the inert-gas calibrations, and the estimated errors involved, has been described elsewhere.[15,16]

Computations

All calculations were performed using the Amsterdam density functional (ADF) program suite.[17] Triple-zeta Slater-type orbital atomic basis sets were employed for all orbitals. Frozen cores were used for all elements (except H), C (1s), Cl (2p) and Ti (2p). A single polarisation function was included for all atoms except Ti. The local density functional of Vosko *et al.*[18] was employed with the correlation correction of Stoll *et al.*[19] and Becke's non-local (gradient) correction[20] to the exchange part of the potential.

Ionisation energies were calculated using Slater's transition-state method.[21] Separate calculations were converged for each ionisation energy. Mulliken population analyses[22] were performed.

The molecular geometry employed was that determined by electron diffraction,[4] with the exception that the Cl–Ti–C–H torsion angle was set to 0° (*i.e.* the symmetry was idealised to C_{3v}).

Results and Discussion

The He I spectrum of $[TiMeCl_3]$ is shown in Fig. 1 and the vertical i.e. are in Table 1. The spectrum differs from that obtained in the previous PE study.[10] Band A was detectable in the previous spectrum, though of very low intensity, but the Cl 3p ionisation region resembled that of $TiCl_4$. We may conclude that $TiCl_4$ was absent from our sample as it gives (amongst others) a sharp band in the He I spectrum at 13.91 eV which is absent in our spectrum.[23–26] Eight bands, A–H, one (D) being a shoulder, are clearly distinguished with ionisation energies

Table 1 Valence molecular orbital eigenvalues, occupations, compositions and ionisation energies for [$TiMeCl_3$]

			Fragment contribution (%)[a]			Ionisation energies/eV	
Orbital	Band label	ε/eV	Ti	Cl	Me	Calc.[b]	Exptl.
$6a_1$		−2.250	52 d, 9 p	7 p	24 $2a_1$ (C)		
7e		−3.144	68 d	20 p			
6e (LUMO)		−3.798	81 d	13 p			
$5a_1$ (HOMO)	A	−7.079	26 d		60 $2a_1$ (C)	10.372	10.63
$1a_2$	B	−7.576		100 p		10.455	11.55
5e	C	−7.872		92 p	5 1e (CH)	10.614	11.95
$4a_1$	D	−8.273	7 d, 5 p	89 p		11.063	12.52
4e	E	−8.457	11 d	86 p		11.224	12.76
3e	F	−9.044	20 d	79 p		11.919	13.09
$3a_1$	G	−9.337	5 d	87 p		12.180	13.55
2e	H	−10.103			91 1e (CH)	13.946	13.99
$2a_1$		−16.778			100 $1a_1$ (CH)	20.850	18.1
1e		−19.899		97 s		22.859	22.6
$1a_1$		−20.106		98 s		23.060	22.6

[a] If >5%. [b] Transition-state method.

Table 2 The r.p.p.i.c.s.s of bands A–H in the PE spectrum of [$TiMeCl_3$]*

	r.p.p.i.c.s. of band							
hν/eV	A	B	C	D	E	F	G	H
22.00	452(9) × 10^2	690(10) × 10^2	141(1) × 10^3	180(2) × 10^3	138(1) × 10^3	204(2) × 10^3	854(10) × 10^2	174(2) × 10^3
24.00	442(7) × 10^2	600(8) × 10^2	110(1) × 10^3	184(1) × 10^3	866(10) × 10^2	156(1) × 10^3	745(9) × 10^2	191(1) × 10^3
25.00	415(8) × 10^2	550(9) × 10^2	107(1) × 10^3	142(1) × 10^3	831(10) × 10^2	139(1) × 10^3	679(10) × 10^2	124(1) × 10^3
28.00	352(6) × 10^2	352(7) × 10^2	669(9) × 10^2	136(1) × 10^3	476(8) × 10^2	846(10) × 10^2	477(8) × 10^2	115(1) × 10^3
30.00	283(5) × 10^2	228(5) × 10^2	454(7) × 10^2	836(7) × 10^2	350(7) × 10^2	567(7) × 10^2	319(6) × 10^2	772(8) × 10^2
32.00	240(5) × 10^2	144(4) × 10^2	293(6) × 10^2	547(6) × 10^2	203(6) × 10^2	359(6) × 10^2	228(5) × 10^2	797(9) × 10^2
34.00	186(4) × 10^2	77(2) × 10^2	151(3) × 10^2	332(4) × 10^2	110(5) × 10^2	196(4) × 10^2	107(3) × 10^2	384(5) × 10^2
36.00	166(3) × 10^2	51(2) × 10^2	106(3) × 10^2	172(3) × 10^2	73(3) × 10^2	146(3) × 10^2	105(3) × 10^2	499(6) × 10^2
38.00	168(3) × 10^2	38(1) × 10^2	77(2) × 10^2	120(2) × 10^2	49(2) × 10^2	112(2) × 10^2	91(2) × 10^2	373(4) × 10^2
40.00	184(3) × 10^2	19(1) × 10^2	70(2) × 10^2	87(2) × 10^2	81(2) × 10^2	141(3) × 10^2	101(3) × 10^2	277(4) × 10^2
41.00	183(4) × 10^2	13(1) × 10^2	62(2) × 10^2	90(3) × 10^2	101(53) × 10^2	207(4) × 10^2	98(3) × 10^2	266(4) × 10^2
42.00	220(3) × 10^2	10(1) × 10^2	60(2) × 10^2	93(2) × 10^2	91(2) × 10^2	214(3) × 10^2	92(2) × 10^2	168(3) × 10^2
43.00	216(3) × 10^2	16(1) × 10^2	55(2) × 10^2	73(2) × 10^2	80(2) × 10^2	215(3) × 10^2	89(2) × 10^2	236(4) × 10^2
45.00	193(4) × 10^2	15(1) × 10^2	49(2) × 10^2	74(2) × 10^2	73(2) × 10^2	190(4) × 10^2	71(2) × 10^2	213(4) × 10^2
50.00	166(4) × 10^2	19(1) × 10^2	42(2) × 10^2	71(3) × 10^2	73(3) × 10^2	172(4) × 10^2	54(2) × 10^2	128(3) × 10^2

* Errors are statistical associated with band-area measurements.

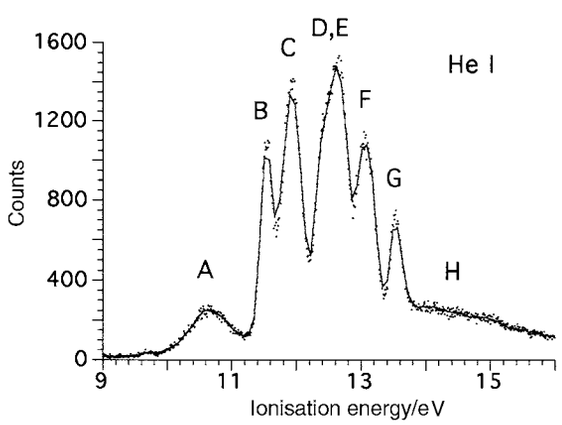

Fig. 1 The He I PE spectrum of [$TiMeCl_3$]

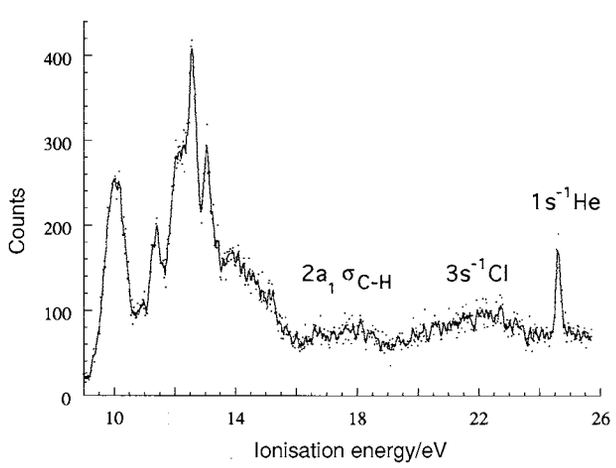

Fig. 2 The He II PE spectrum of [$TiMeCl_3$]

below 16 eV. The He II spectrum (Fig. 2) reveals two further broad ionisation features centred around 18.1 and 22.6 eV. Fig. 3 shows spectra acquired with synchrotron radiation of energy 22, 35 and 43 eV. These reveal striking changes in the relative intensities of the bands. Bands B–E decline in relative intensity with increase in photon energy, F and G initially fall but then recover at higher photon energy, A shows a general rise in relative intensity, whereas H rises but then falls.

Branching ratios for bands A–H are plotted in Fig. 4. Individual r.p.p.i.c.s. are given in Fig. 5. These data are also given in Tables 2 and 3. Theoretical atomic photoionisation cross-sections are shown in Fig. 6.[27] These are calculated for direct one-electron photoionisation and do not include allowance for any resonance processes which are frequently found for transition-metal complexes.[11]

For a detailed band assignment a molecular orbital scheme is required for the molecule. Fig. 7 presents a qualitative scheme based on the density functional calculations, the results of

Table 3 Branching ratios for bands A–H of [$TiMeCl_3$] as a function of photon energy

	b.r. of band							
hν/eV	A	B	C	D	E	F	G	H
22.00	0.043(1)	0.066(1)	0.135(2)	0.177(2)	0.133(2)	0.196(2)	0.082(1)	0.167(2)
24.00	0.051(1)	0.069(1)	0.127(1)	0.164(2)	0.100(2)	0.180(1)	0.086(1)	0.221(2)
25.00	0.055(1)	0.073(1)	0.141(2)	0.180(2)	0.110(2)	0.185(1)	0.090(1)	0.164(2)
28.00	0.068(1)	0.068(1)	0.130(2)	0.162(2)	0.092(2)	0.164(1)	0.092(1)	0.222(3)
30.00	0.081(2)	0.066(2)	0.131(2)	0.158(2)	0.101(2)	0.163(1)	0.092(2)	0.208(3)
32.00	0.092(2)	0.055(2)	0.113(2)	0.128(2)	0.078(3)	0.138(2)	0.088(2)	0.307(3)
34.00	0.135(2)	0.056(2)	0.109(3)	0.124(3)	0.079(3)	0.142(2)	0.077(2)	0.277(4)
36.00	0.131(1)	0.041(2)	0.084(2)	0.094(2)	0.058(3)	0.115(3)	0.083(2)	0.394(5)
38.00	0.168(3)	0.038(2)	0.077(2)	0.088(2)	0.050(3)	0.113(3)	0.092(2)	0.375(5)
40.00	0.190(1)	0.020(2)	0.072(2)	0.093(3)	0.085(3)	0.146(3)	0.105(3)	0.287(5)
41.00	0.179(9)	0.012(2)	0.061(2)	0.091(3)	0.099(4)	0.202(4)	0.096(3)	0.260(5)
42.00	0.240(4)	0.011(2)	0.064(2)	0.078(2)	0.098(4)	0.230(4)	0.099(2)	0.181(3)
43.00	0.220(9)	0.016(2)	0.056(2)	0.079(2)	0.081(4)	0.218(4)	0.090(2)	0.239(4)
45.00	0.220(1)	0.017(1)	0.056(2)	0.085(3)	0.083(5)	0.215(5)	0.081(3)	0.242(5)
50.00	0.230(2)	0.027(3)	0.058(3)	0.098(4)	0.100(6)	0.237(6)	0.074(3)	0.176(5)

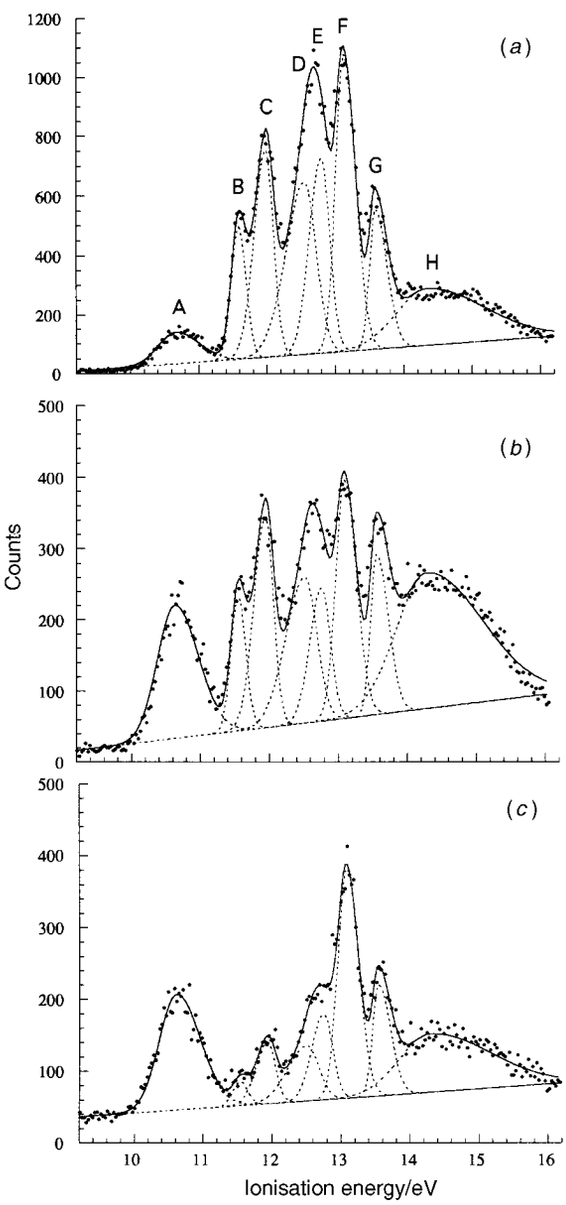

Fig. 3 The PE spectra of [$TiMeCl_3$] acquired with photon energies of (*a*) 22, (*b*) 35 and (*c*) 43 eV

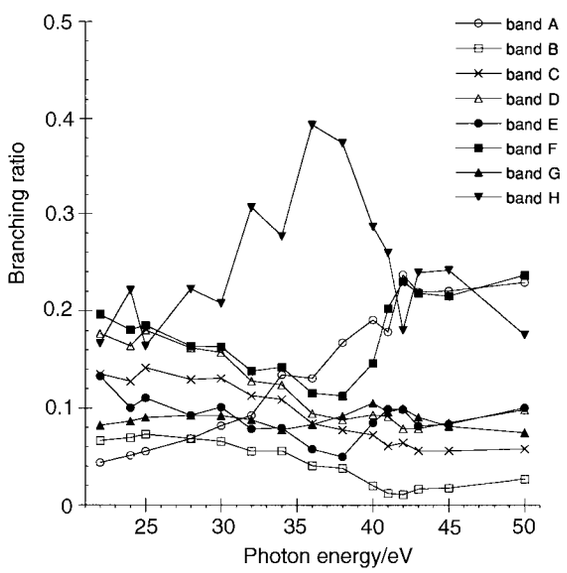

Fig. 4 Branching ratios for bands A–H in the PE spectrum of [$TiMeCl_3$]

which are given in Table 1. The transition-state calculations in this case suggest the same ordering for the Kohn–Sham one-electron energies and the associated ionisation energies.

Band B shows classic Cl 3p cross-section behaviour with a very steep initial decrease and a shallow minimum reminiscent of the t_1 band of $TiCl_4$.[26] The minimum at a photon energy of 42 eV is assigned to the Cl 3p Cooper minimum[28] which is predicted to occur at a PE kinetic energy of *ca.* 30 eV.[27] Band B has an i.e. of 11.55 eV so here the kinetic energy of the minimum is 30.5 eV, in excellent agreement with the prediction. Band B may be confidently assigned to ionisation from the $1a_2$ level which, from symmetry considerations, must be localised on the Cl p_π atomic orbitals. Band C is double the intensity of B and has a very similar cross-section profile, though it shows no Cooper minimum, rather a flat profile above 40 eV. It can be assigned to the 5e level, for which a very high halogen content can be inferred.

Band A at 21 eV is the least intense band but at 50 eV it is one of the most intense bands (along with F). It shows a minimum in its cross-section around 37 eV and maximum around 42 eV. From the one-electron cross-section profiles (Fig. 6) the relative rise in intensity can be attributed to Ti 3d character in the orbital from which ionisation is occurring. However the minimum is too pronounced and in the wrong region for a Cl 3p Cooper minimum. It is most likely associated with a Ti $3p \longrightarrow 3d$ resonance excitation followed by super Coster–Kronig decay resulting in ejection of electrons with 3d character.[11] A cross-section modification, with a Fano profile,[29,30] is expected for this complex process in the region of the Ti 3p

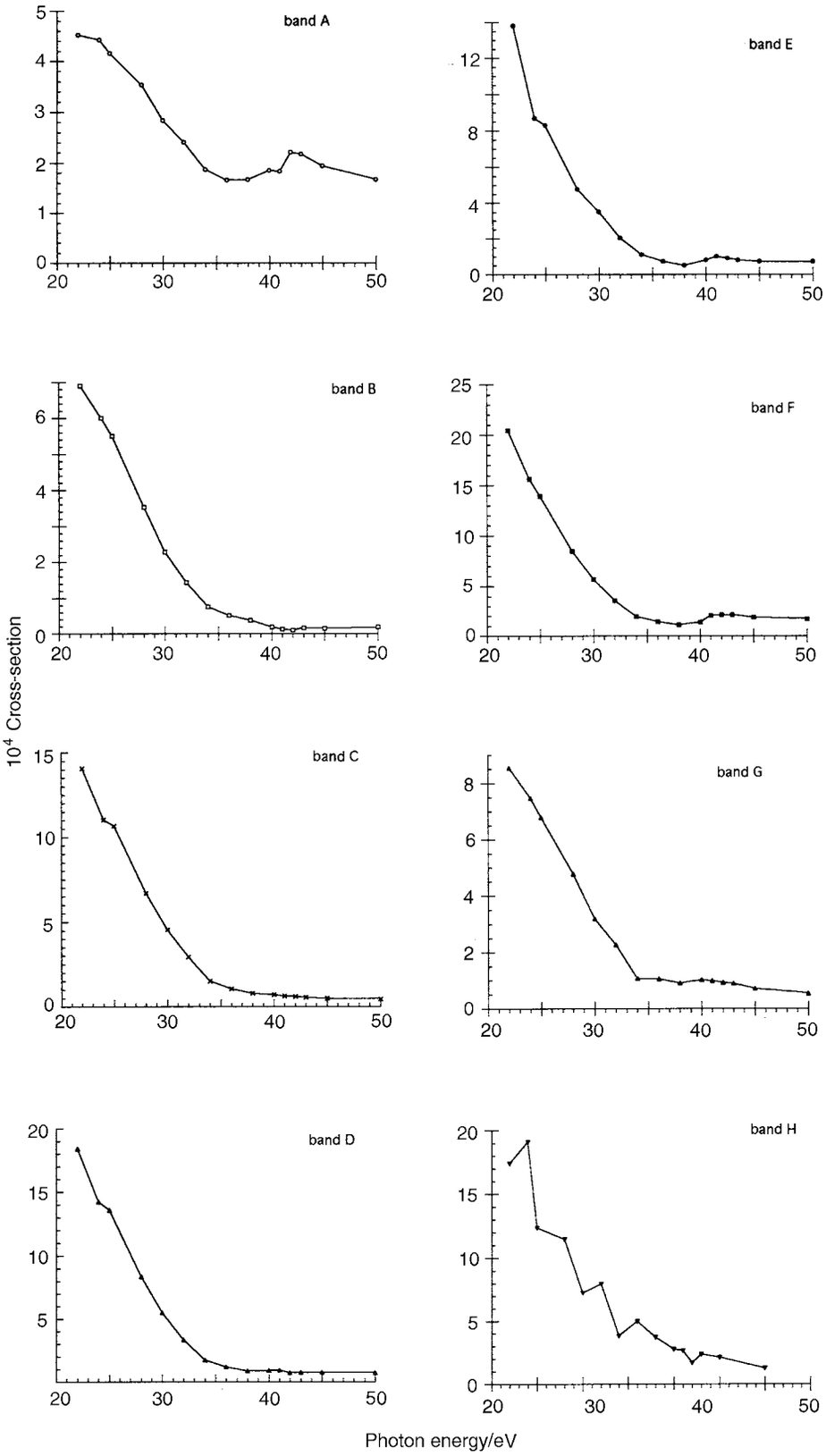

Fig. 5 Relative partial photoionisation cross-sections for bands A–H in the PE spectrum of [$TiMeCl_3$]

absorption edge; Ti 3p AOs ionise at 38 ($^2P_{\frac{3}{2}}$) and 39 ($^2P_{\frac{1}{2}}$) eV. In a variable photon-energy study of $TiCl_4$ the $2t_2$ and 1e bands were found to have a minimum at 38 eV and a maximum at 49 eV.[26] Band A is thus associated with an orbital of Ti 3d character, and negligible Cl character; it may be assigned to ionisation of the $5a_1$ highest occupied molecular orbital (HOMO) associated with the Ti–C bond.

Bands E and F show a fall in cross-section between 20 and 35 eV very similar to that of B, demonstrating their Cl 3p character. However they also show a minimum at 38 eV and a maximum around 41 eV rather than the Cooper minimum characteristic of Cl 3p ionisations. This resonance feature parallels that of band A and indicates Ti 3d character. Thus these bands show features characteristic of both Cl 3p orbitals and Ti 3d orbitals, the former being predominant. The intensity of band F suggests assignment to the 3e ionisation. The

Table 4 Gross atomic charges and Mulliken populations for atomic orbitals

Ti*		Cl		C		H	
Orbital	Population	Orbital	Population	Orbital	Population	Orbital	Population
s	2.08	s	1.99	s	1.14	s	0.99
p	6.31	p	5.35	p	2.78	p	0.08
d	2.34	d	0.03	d	0.02		
Charge	+1.27		−0.37		+0.05		−0.07

* Titanium populations include the 3s and 3p core electrons.

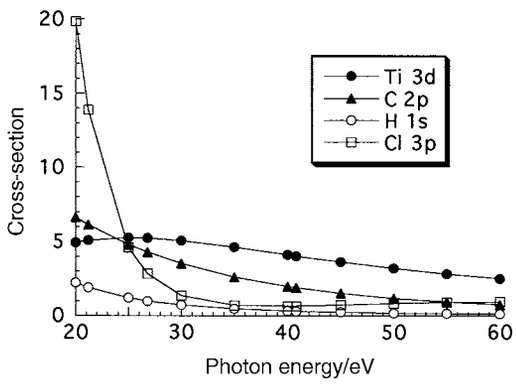

Fig. 6 Theoretical atomic ionisation cross-sections for Ti 3d, H 1s, C 2p and Cl 3p orbitals[27]

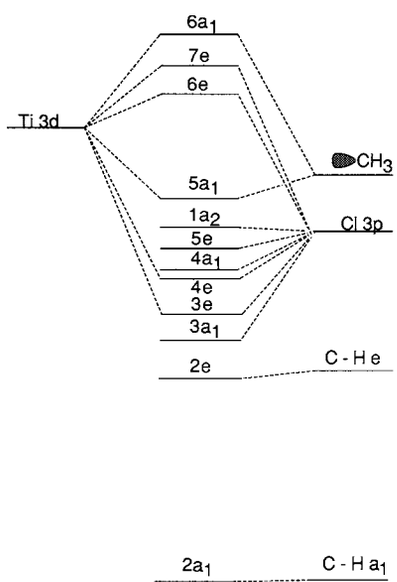

Fig. 7 Molecular orbital scheme for [$TiMeCl_3$]

behaviour of bands G and D is intermediate between that of B and C and that of E and F. Band G is, on average, approximately half the intensity of F and is assigned to the $3a_1$ ionisation. Assignment of bands D and E is problematic as they overlap extensively. The fitting suggests that D is somewhat more intense than E whereas the cross-section variation gives E relatively more Ti 3d character. On balance the ionisation order suggested by the calculation is probably correct, and the fitting less than ideal, so band D is assigned to the $4a_1$ ionisation and E to that for the 4e level. It is worth noting that e ionisations lead to orbitally degenerate states which, if of bonding character, may well be split by Jahn–Teller distortion; no account of this is taken in the transition-state ionisation calculations.

The position, shape and cross-section behaviour of band H suggest that it be assigned to the C–H 2e ionisation band. It is the most intense band at photon energies between 30 and 40 eV; in this region the C 2p character of the orbital dominates the cross-section variation. As noted in the Experimental section, the band width is large and the band profile difficult to determine, making the intensity data less certain. The branching ratio variation is therefore less smooth than that found for other bands. Ionisation bands of C–H localised degenerate orbitals are often found to show Jahn–Teller splitting and this may also be the case for band H though, as mentioned in the Experimental section, the poor definition of the band shape means this cannot be ascertained. Within these limitations, no metal-like $3p \longrightarrow 3d$ resonance enhancement of the cross-section may be detected for this band suggesting that the metal character of the ionising MO is very low.

Subsequent bands at 18.1 and 22.6 eV (Fig. 2) are assigned to ionisation from the methyl $2a_1$ orbital and the Cl 3s-based MOs ($1a_1$ + 1e) respectively.

Comparison with theory

The electronic structure of [$TiMeCl_3$] has been studied repeatedly by a number of groups.[8,31–33] Indeed it has been used as a testing ground for effective core potentials and basis sets.[31] All calculations give reasonable agreement with the electron-diffraction data. However none of them includes details of one-electron energy levels or any other method of estimating an ionisation-energy ordering or the character of the ionising MO. We, therefore, undertook a density functional study to obtain a description of the bonding and to estimate i.e. These results are shown in Table 1.

Though there is good agreement between several of the experimental and theoretical i.e.s, all of the mainly Cl-localised ionisations are calculated by the transition-state method to have i.e. 1–1.5 eV lower than those observed. The i.e. ordering, however, where it is independently established from the cross-section and branching ratio data, is in good agreement with that predicted.

Comparison of the experimentally determined r.p.p.i.c.s. with the MO compositions in Table 1 reveals that the atomic character of the MOs is in good agreement with the cross-section variations of the related PE bands. The 26% Ti 3d contribution to the $5a_1$ HOMO ties in with the $p \longrightarrow d$ resonant enhancement of the cross-section of the associated PE band (band A) in the region of the Ti 3p subshell ionisation potentials. Of the nine mainly Cl 3p-based MOs ($3a_1$–$1a_2$) only the $1a_2$ and 5e orbitals have less than 5% Ti 3d character. The mixed Ti 3d–Cl 3p nature of the $3a_1$–$4a_1$ orbitals has been discussed above. Symmetry constraints preclude any Ti 3d contribution to the $1a_2$ MO, and the 5e orbital also retains the nodal characteristics of the parent $1t_1$ ionisation in $TiCl_4$, resulting in unfavourable overlap with the central atom. The 2e orbital, which is C–H localised, shows no sign of any significant Ti 3d content in its cross-section behaviour, in agreement with the 4% Ti 3d contribution found in the calculation. This is consistent with the now well established lack of distortion of the methyl group.

Table 4 presents the gross charges on each atom. Mulliken analyses generally do not produce the formal charges assigned

by oxidation-state criteria, but the data in Table 4 indicate an appreciable difference between the charges on Ti and C, with Ti being +1.218 with respect to C. This may be taken as evidence of significant polarity in the Ti–C bond. That there is appreciable covalency in the Ti–C bond is evidenced by the atomic overlap population, which at +0.420 electron indicates that overall Ti–C interaction is significantly bonding, as is the Ti–Cl interaction (+0.457 electron).

Electronic structure and chemical reactivity

It is instructive to compare the MO diagram (Fig. 7) and the ionisation energies (Table 1) we have determined for $[TiMeCl_3]$ with those reported in an earlier study of $TiCl_4$.[26] Whilst direct correlation of individual MOs is precluded on account of the different symmetries, certain comparisons are valid. For $TiCl_4$ the Ti–Cl bonding MOs lie at energies in the range −10 to −11 eV, the corresponding Ti–Cl orbitals in $[TiMeCl_3]$ being somewhat higher at −7.5 to −9.5 eV. In each molecule the lowest unoccupied molecular orbital (LUMO) consists of antibonding Ti–Cl orbitals of mainly metal character. The relatively low energy of the LUMO, −5.7 eV in $TiCl_4$ and −3.8 eV in $[TiMeCl_3]$, is responsible for the Lewis-acidic nature of the titanium(IV) centre in each case, with both $TiCl_4$ and $[TiMeCl_3]$ readily forming adducts with mono- and bi-dentate donors such as bipyridyl, ether and $Me_2ECH_2CH_2EMe_2$ (E = N or P),[2,34–36] in which the Ti–Cl bonds are generally observed to be longer than in the parent molecule.

In the case of $[TiMeCl_3]$, however, a second type of reactivity is apparent. The relatively high energy level of the HOMO (−7.1 eV) [*cf.* $TiCl_4$ (−9.1 eV)], which corresponds to the Ti–C bonding orbital, possibly in concert with the relatively polar nature of the TiMe moiety (Table 4), leads to a high lability of the Ti–C bond. Thus oxidation of $[TiMeCl_3]$ proceeds by insertion to give $[TiCl_3(OMe)]$;[37] the reagents $HgCl_2$, $SnCl_4$ and $AlCl_3$ all exchange the methyl ligand for chloride,[38] whilst treatment with protonic species results in the ready evolution of methane.[37] Rupture of the Ti–C bond with evolution of methane also appears to be the predominant decomposition pathway for $[TiMeCl_3]$.

Conclusion

A pure sample of $[TiMeCl_3]$ may be prepared by treating $TiCl_4$ with $ZnMe_2$ but careful monitoring is required to ensure that the reaction goes to completion. This required a 15% molar excess of $ZnMe_2$. The PE spectrum shows substantial intensity changes over the photon-energy range 22–50 eV which enabled complete assignment of the ion states and the character of the associated orbitals. These were in good agreement with predictions from density functional theory. The Ti–C bond was shown to be covalent but polar. The number of primary Cl 3p-based orbitals showing Ti 3d contributions supports a model with Cl $3p_\pi$ donation to the Ti 3d orbitals.

Acknowledgements

We thank the EPSRC for financial support, the Accademia dei Lincei di Roma for a fellowship (to M. D. S.), the Royal Society for an equipment grant (to N. K.) and Jesus College, Oxford for a Research Fellowship (to G. S. M.).

References

1 A. Berry, Z. Dawoodi, A. E. Derome, J. M. Dickinson, A. J. Downs, J. C. Green, M. L. H. Green, P. M. Hare, M. P. Payne, D. W. H. Rankin and H. E. Robertson, *J. Chem. Soc., Chem. Commun.*, 1986, 520.
2 Z. Dawoodi, M. L. H. Green, V. S. B. Mtetwa, K. Prout, A. J. Schultz, J. M. Williams and T. F. Koetzle, *J. Chem. Soc., Dalton Trans.*, 1986, 1629.
3 M. Yu. Antipin, S. I. Troyanov, Yu. T. Struchkov and L. S. Bresler, *Metalloorg. Khim.*, 1988, **1**, 111.
4 P. Briant, J. Green, A. Haaland, H. Møllendal, K. Rypdal and J. Tremmel, *J. Am. Chem. Soc.*, 1989, **111**, 3434.
5 M. L. H. Green and A. K. Hughes, *J. Chem. Soc., Chem. Commun.*, 1991, 1231.
6 D. C. McKean, G. P. McQuillan, I. Torto, N. C. Bednall, A. J. Downs and J. M. Dickinson, *J. Mol. Struct.*, 1991, **247**, 73.
7 R. L. Williamson and M. B. Hall, *J. Am. Chem. Soc.*, 1988, **110**, 4428.
8 R. Krömer and W. Thiel, *Chem. Phys. Lett.*, 1992, **189**, 105.
9 S. Berger, W. Bock, G. Frenking, V. Jonas and F. Muller, *J. Am. Chem. Soc.*, 1995, **117**, 3820.
10 M. Basso-Bert, P. Cassoux, F. Crasnier, D. Gervais, J.-F. Labarre and P. De Loth, *J. Organomet. Chem.*, 1977, **136**, 201.
11 J. C. Green, *Acc. Chem. Res.*, 1994, **27**, 131.
12 S. Berger, W. Bock, G. Frenking, V. Jonas and F. Müller, *J. Am. Chem. Soc.*, 1995, **117**, 3820.
13 S. G. McGrady, A. J. Downs, N. C. Bednall, D. C. McKean, W. Thiel, V. Jonas, G. Frenking and W. Scherer, unpublished work.
14 J. F. Hanlan and J. D. McCowan, *Can. J. Chem.*, 1972, **50**, 747.
15 C. N. Field, D. Phil. Thesis, University of Oxford, 1995.
16 G. Cooper, J. C. Green, M. P. Payne, B. R. Dobson and I. H. Hiller, *J. Am. Chem. Soc.*, 1987, **109**, 3836.
17 ADF⟨1.1.4⟩, Department of Theoretical Chemistry, Vrije Universiteit, Amsterdam, 1995.
18 S. H. Vosko, L. Wilk and M. Nusair, *Can. J. Phys.*, 1980, **58**, 1200.
19 H. Stoll, C. M. E. Pavlidou and H. Preuss, *Theor. Chim. Acta*, 1978, **49**, 143.
20 A. Becke, *Phys. Rev. A*, 1988, **38**, 3098.
21 J. S. Slater, *The Calculation of Moleclar Orbitals*, Wiley, New York, 1979.
22 R. S. Mulliken, *J. Chem. Phys.*, 1955, **23**, 1833.
23 J. C. Green, M. L. H. Green, P. J. Joachim, A. F. Orchard and D. W. Turner, *Philos. Trans. R. Soc. London, Ser. A*, 1970, **268**, 111.
24 R. G. Egdell, A. F. Orchard, D. R. Lloyd and N. V. Richardson, *J. Electron Spectrosc. Relat. Phenom.*, 1977, **12**, 415.
25 G. M. Bancroft, E. Pellach and J. S. Tse, *Inorg. Chem.*, 1982, **21**, 2950.
26 B. E. Bursten, J. C. Green, N. Kaltsoyannis, M. A. MacDonald, K. H. Sze and J. S. Tse, *Inorg. Chem.*, 1994, **33**, 5086.
27 J. Yeh, *At. Data Nucl. Data Tables*, 1993.
28 J. W. Cooper, *Phys. Rev. Lett.*, 1964, **13**, 762.
29 U. Fano, *Phys. Rev.*, 1961, **124**, 1866.
30 U. Fano and J. W. Cooper, *Phys. Rev. A*, 1965, **137**, 1364.
31 V. Jonas, G. Frenking and M. T. Reetz, *J. Comput. Chem.*, 1992, **13**, 919.
32 N. Rösch and P. Knappe, *ACS Symp. Ser.*, 1989, **394**, 37.
33 R. L. Williamson and M. B. Hall, *ACS Symp. Ser.*, 1989, **394**, 17.
34 F. A. Cotton and G. Wilkinson, *Advanced Inorganic Chemistry*, 5th edn., Wiley-Interscience, New York, 1988, p. 657.
35 K.-H. Thiele, *Pure Appl. Chem.*, 1992, **30**, 575.
36 R. J. H. Clarke, S. Moorhouse and D. A. Stockwell, *J. Organomet. Chem. Libr.*, 1977, **3**, 223.
37 C. Beerman and H. Bestian, *Angew. Chem.*, 1959, **71**, 618.
38 E. H. Ademan, *J. Polym. Sci., Polym. Symp.*, 1968, **16**, 3643.

Received 19*th August* 1996; *Paper* 6/05753E